Center for Turbulence Research
Proceedings of the Summer Program 1994

Pdf modeling for premixed turbulent combustion based on the properties of iso-concentration surfaces

By L. Vervisch[1], W. Kollmann[2], K. N. C. Bray[3], AND T. Mantel[4]

In premixed turbulent flames the presence of intense mixing zones located in front of and behind the flame surface leads to a requirement to study the behavior of iso-concentration surfaces defined for all values of the progress variable (equal to unity in burnt gases and to zero in fresh mixtures). To support this study, some theoretical and mathematical tools devoted to level surfaces are first developed. Then a database of direct numerical simulations of turbulent premixed flames is generated and used to investigate the internal structure of the flame brush, and a new pdf model based on the properties of iso-surfaces is proposed.

1. Introduction

In order to improve existing models of premixed turbulent combustion (Borghi 1988), it is necessary to build a bridge from zones where intense reactive activity occurs in laminar flamelets to the more distributed reaction zones found in front of and behind these propagating flame surfaces. This is especially true if one wishes to predict not only the global structure of the flame, but also the concentration level of pollutants using any probabilistic approach. Indeed, the turbulent mixing acting in the preheat zone can strongly influence the structure of the entire flame; therefore, a description of this mixing, together with descriptions of chemical sources or of topological properties of the flame surface, must be used to account for their mutual interactions.

The objective of this work is the development of a formalism, adapted to premixed turbulent combustion modeling, which brings the possibility to treat simultaneously flamelet behavior and out-of-flamelet mixing. This is a crucial point because they both interact to control the properties of the propagation velocity of the flame front (Bray 1990, Pocheau 1992).

To account for the possible presence of flamelets, the flame surface density approach (Marble and Broadwell 1977) is extended to the concept of a surface density function and coupled with probability density function (pdf) method (Pope 1985).

1 LMFN-INSA, URA - CNRS 230 - CORIA, France
2 MAE, University of California at Davis
3 Cambridge University, Engineering Department, U.K.
4 Center for Turbulence Research

First some theoretical considerations and mathematical tools concerning iso-surfaces in fluid mechanical problems are developed. In Section 2.1 a useful mathematical relation between surface and volume integrals is introduced which has several applications of theoretical and practical importance. It is used first (Section 2.2) to establish the transport equation for global variables such as the total surface area of iso-concentration surfaces, and from this the classical expression for premixed flame stretch is recovered. The solution of the area equation for a material surface is proposed (Section 2.3). In particular, it is shown that the combination of the introduced mathematical relation with Lagrangian variables leads to an expression for the area of a temporally evolving level surface, which only requires the integration over the surface at a fixed time. In Section 2.4 the same formalism is used in conjunction with an integral transform for the computation of the area of iso-surfaces without computing the location of the surfaces. This leads to a novel method for the efficient computation of the surface area of iso-surfaces, which is superior to triangulation methods that keep track of the connectedness of the surface. Finally, the concept of a surface density function (sdf) emerges (Section 2.5) along with its transport equation, and a unified treatment of pdf and sdf equations is discussed (Section 2.6).

A direct numerical simulation (DNS) database of premixed turbulent combustion is developed and used in Section 3 to study the internal structure of the turbulent flame, and various key quantities identified in Section 2 are analyzed. In particular, the behavior of quantities integrated over iso-concentration surfaces is carefully examined within the inner structure of the premixed flame, for surfaces located between fresh and burnt gases.

The pdf formulation reduces the modeling difficulties emerging when the mean burning rate needs to be estimated to the finding of a closed expression for the small scales mixing which depends on the distribution of the gradient of the reactive species along their iso-surfaces. The surface density function contains information about these gradients, especially within the flamelet zone. Based on this remark, an attempt to couple the pdf with the sdf is proposed in Section 4, and the resulting modeled expressions are tested against their exact values extracted from the DNS.

2. Transport equations for surfaces

2.1 Introduction

In multi-composition fluid mechanical problems, the starting point for studying the quantities characterizing the physical properties of the flow field are usually budget equations for volume integrals over a volume of fluid $\mathcal{D}$. To derive equations for the corresponding properties of iso-surfaces, it is necessary to link volume integrals and integrals over these surfaces. The following theorem of geometric measure theory (Maz'ja 1985, ch.1.2.4, p.37, Constantin 1992) provides the bridge between volume integrals and integrals over iso-surfaces.

Theorem: Let $F(\underline{x})$ be a Borel-measurable nonnegative function on $\mathcal{D} \subseteq R^3$ open. Let $\Phi(\underline{x}) \in C^\infty(\mathcal{D})$. Then

$$\int_{\mathcal{D}} d\underline{x} F(\underline{x}) |\nabla \Phi(\underline{x})| = \int_0^\infty d\varphi \int_{S_\Phi(\varphi)} dA(\underline{x}) F(\underline{x}) \quad , \tag{1}$$

where $S_\Phi(\varphi) = \{\underline{x} \in \mathcal{D} : \Phi(\underline{x}) = \varphi\}$ is the level surface or iso-surface of the field $\Phi(\underline{x})$ on which $\Phi(\underline{x})$ takes the value φ. This condition specifies that the level surfaces are contained in the domain $\mathcal{D}$ (no intersection of the surfaces with the domain boundary). It is possible to remove this restriction, but this case will not be pursued here.

The co-area formula follows at once if the function $F(\underline{x})$ is specified as:

$$F(\underline{x}) = f(\underline{x}) \delta(\Phi(\underline{x}) - \varphi) \quad ,$$

where $\delta(\Phi(\underline{x}) - \varphi)$ is the diract delta function, leading to the desired result

$$\int_{\mathcal{D}} d\underline{x} f(\underline{x}) |\nabla \Phi(\underline{x})| \delta(\Phi(\underline{x}) - \varphi) = \int_{S_\Phi(\varphi)} dA(\underline{x}) f(\underline{x}) \quad . \tag{2}$$

2.2 Transport equation for global variables

The total area of level surfaces is an example of a global variable. In general, a global variable is defined by

$$\mathcal{F}_\Phi(\varphi, t) \equiv \int_{S_\Phi(\varphi)} dA(\underline{x}) f(\underline{x}, t) \quad , \tag{3}$$

where the unspecified function $f(\underline{x}, t)$ must satisfy the conditions of the above theorem. In most cases it will be a smooth function of location and time to allow differentiation. Application of Eq. 2 to Eq. 3 and differentiation with respect to time leads to the transport equation for $\mathcal{F}_\Phi$ in terms of volume integrals

$$\frac{\partial \mathcal{F}_\Phi}{\partial t}(\varphi, t) + \frac{\partial}{\partial \varphi} \mathcal{L}_\Phi = S_f + S_\Phi \quad . \tag{4}$$

Three contributions determine the time rate of change of the global variable $\mathcal{F}_\Phi(\varphi, t)$: a convective transport term in scalar space and two source terms. The flux in scalar space is defined by

$$\mathcal{L}_\Phi \equiv \int_{\mathcal{D}} d\underline{x} \delta(\Phi - \varphi) |\nabla \Phi| f(\underline{x}, t) \frac{\partial \Phi}{\partial t} \quad , \tag{5}$$

the source due to the evolution of $f(\underline{x}, t)$ is

$$S_f(\varphi, t) \equiv \int_{\mathcal{D}} d\underline{x} \delta(\Phi - \varphi) |\nabla \Phi| \frac{\partial f}{\partial t} \quad , \tag{6}$$

and finally the source due to the evolution of the scalar field defining the level surfaces is

$$S_\Phi(\varphi,t) \equiv \int_{\mathcal{D}} d\underline{x}\delta(\Phi-\varphi)f(\underline{x},t)\frac{\partial|\nabla\Phi|}{\partial t} \quad . \tag{7}$$

The co-area formula Eq. 2 can be applied once more to obtain an equivalent version in terms of surface integrals

$$\frac{\partial\mathcal{F}_\Phi}{\partial t}(\varphi,t) = \int_{S_\Phi(\varphi)} dA\left(\frac{D^s f}{Dt} + f\frac{D^s}{Dt}\log(|\nabla\Phi|) + f\frac{\partial v_\alpha^s}{\partial x_\alpha}\right) \quad , \tag{8}$$

where $\frac{D^s}{Dt}$ is the time rate of change following points on the level surface. The time rate of change of the global variable $\mathcal{F}_\Phi$ is seen to be caused by the change of the function $f(\underline{x},t)$ on the level surface, the time rate of change of $\log(|\nabla\Phi|)$ on the level surface, and the surface divergence of flow velocity.

The dynamic equations for global variables can be established once the transport equations for the scalar $\Phi(\underline{x},t)$ defining the level surfaces and the scalar $f(\underline{x},t)$ are known. In the case of flames, the transport equation for a reactive scalar field may be written:

$$\frac{D\Phi}{Dt} = \Omega_\Phi \quad , \tag{9}$$

where $D/Dt = \partial/\partial t + \underline{v}.\nabla$ is the substantial derivative and

$$\Omega_\Phi = \frac{1}{\rho}\frac{\partial}{\partial x_\alpha}\left(\rho\Gamma\frac{\partial\Phi}{\partial x_\alpha}\right) + \dot{W}_\Phi(\Phi) \quad , \tag{10}$$

denotes the imbalance of diffusion and source terms. The transport equation for f is assumed to be in the generic form

$$\rho\left(\frac{\partial f}{\partial t} + v_\alpha\frac{\partial f}{\partial x_\alpha}\right) = \frac{\partial}{\partial x_\alpha}\left(\rho\lambda\frac{\partial f}{\partial x_\alpha}\right) + \rho\dot{W}_f(f) \quad . \tag{11}$$

The iso-surfaces are defined implicitly as solution of

$$S_\Phi(\varphi,t) \equiv \Phi(\underline{x},t) - \varphi = 0 \quad , \tag{12}$$

and the unit normal vector of the iso-surface is defined by

$$n_\alpha \equiv -\frac{1}{|\nabla\Phi|}\frac{\partial\Phi}{\partial x_\alpha} \quad . \tag{13}$$

The surfaces move in their normal direction, with the velocity

$$v_\alpha^s = v_\alpha + Vn_\alpha \quad . \tag{14}$$

The relative progression velocity V of the level surfaces is determined by the imbalance Eq. 10 of diffusion and source term in Eq. 9:

$$V = \frac{1}{\rho|\nabla\Phi|}\frac{\partial}{\partial x_\alpha}(\rho\Gamma\frac{\partial\Phi}{\partial x_\alpha}) + \frac{1}{|\nabla\Phi|}\dot{W}_\Phi = \frac{1}{|\nabla\Phi|}\Omega_\Phi \quad . \tag{15}$$

The dynamic equation for the global variable $\mathcal{F}_\Phi$ then follows in terms of volume integrals as

$$\begin{aligned}\frac{\partial\mathcal{F}_\Phi}{\partial t} = &\int_{\mathcal{D}} d\underline{x}\,\delta(\Phi-\varphi)|\nabla\Phi|\left[\frac{1}{\rho}\frac{\partial}{\partial x_\alpha}\left(\rho\lambda\frac{\partial f}{\partial x_\alpha}\right) + \dot{W}_f + f\left(\frac{\partial v_\alpha}{\partial x_\alpha} - n_\alpha n_\beta\frac{\partial v_\beta}{\partial x_\alpha}\right)\right] \\ &+ \int_{\mathcal{D}} d\underline{x}\,\delta(\Phi-\varphi)|\nabla\Phi|\left[\left(\frac{1}{\rho}\frac{\partial}{\partial x_\alpha}\left(\rho\Gamma\frac{\partial\Phi}{\partial x_\alpha}\right) + \dot{W}_\Phi\right)\frac{\partial n_\alpha f}{\partial x_\alpha}\right] \quad .\end{aligned} \tag{16}$$

This is one of several equivalent versions of the dynamic equation for the global variable $\mathcal{F}_\Phi(\varphi,t)$ in variable density turbulence. The equation for the surface area $A_\Phi(\varphi,t)$ is obtained by choosing $f=1$ (see Eq. 3)

$$\frac{\partial\mathcal{A}_\Phi}{\partial t} = \int_{\mathcal{D}} d\underline{x}\,\delta(\Phi-\varphi)\left[|\nabla\Phi|\left(\frac{\partial v_\alpha}{\partial x_\alpha} - n_\alpha n_\beta\frac{\partial v_\beta}{\partial x_\alpha}\right) + \left(\frac{1}{\rho}\frac{\partial}{\partial x_\alpha}\left(\rho\Gamma\frac{\partial\Phi}{\partial x_\alpha}\right) + \dot{W}_\Phi\right)\frac{\partial n_\alpha}{\partial x_\alpha}\right] \tag{17}$$

The corresponding equation in terms of surface integrals can easily be obtained from Eq. 17 by using Eq. 2. In particular, the surface stretch

$$\mathcal{H}(t) = \frac{1}{\mathcal{A}_\Phi}\frac{d\mathcal{A}_\Phi}{dt} \quad , \tag{18}$$

may be cast in the form:

$$\mathcal{H}(t) = \frac{1}{\mathcal{A}_\Phi}\left(\mathcal{I}_1 + \mathcal{I}_2\right) \quad , \tag{19}$$

where

$$\begin{aligned}\mathcal{I}_1 &= \int_{S_\Phi(\varphi)} dA(\underline{x})\phi_s(\underline{x},t) \quad , \\ \mathcal{I}_2 &= \int_{S_\Phi(\varphi)} dA(\underline{x})V(\underline{x},t)\frac{\partial n_\alpha}{\partial x_\alpha} \quad .\end{aligned} \tag{20}$$

In Eq. 20 ϕ_s is a notation for the in-plane strain rate:

$$\phi_s = \frac{\partial v_\alpha}{\partial x_\alpha} - n_\alpha n_\beta\frac{\partial v_\beta}{\partial x_\alpha} \quad , \tag{21}$$

and the imbalance between reactive and diffusive effects Ω_Φ has been written in terms of the relative progression velocity V by using Eq. 10. When the scalar $\Phi(\underline{x},t)$ denotes the progress variable used in premixed combustion ($\Phi = 0$ in fresh gases and $\Phi = 1$ in burnt gases), then by choosing as iso-surface the surface corresponding to the value of the progress variable used to locate the flame front, the well-known result is found that flame stretch is directly related to both contributions of strain rate acting along the flame front ($\mathcal{I}_1$) and curvature linked with propagation of the premixed flame ($\mathcal{I}_2$) (Candel and Poinsot 1990).

Inspection of Eq. 17 shows that the surface area changes due to the strain rate in the tangential plane of the surface caused by the motion of the fluid and the dynamic change of the scalar field defining the level surface. Both phenomena may increase or decrease the surface area. The dynamics of the scalar variable defining the level surface appear in Eq. 17 as molecular diffusion and the source term. It is clear that both may be positive or negative, hence may increase or decrease the surface area as time evolves. The molecular diffusion term can be analyzed in more detail for incompressible flows with constant diffusivity Γ, since it is then proportional to

$$\frac{1}{|\nabla\Phi|}\triangle\Phi\frac{\partial n_\alpha}{\partial x_\alpha} = \frac{\partial n_\alpha}{\partial x_\alpha}\frac{\partial n_\beta}{\partial x_\beta} + \frac{\partial n_\gamma}{\partial x_\gamma}\frac{n_\alpha n_\beta}{|\nabla\Phi|}\frac{\partial^2\Phi}{\partial x_\alpha \partial x_\beta} \quad .$$

The first term on the right side is purely geometrical since it only depends on the mean curvature H

$$H = -\frac{1}{2}\frac{\partial n_\alpha}{\partial x_\alpha} \quad ,$$

whereas the second term depends on the variation of the defining scalar normal to the level surface

$$\frac{\partial\Phi}{\partial n} = \underline{n}\cdot\nabla\Phi \quad ,$$

and it follows that

$$\frac{1}{|\nabla\Phi|}\triangle\Phi\frac{\partial n_\alpha}{\partial x_\alpha} = 4H^2 - 2\frac{H}{|\nabla\Phi|}\frac{\partial^2\Phi}{\partial n^2}$$

holds, which proves that the effect of molecular diffusion on the surface area is not definite: The first term on the right side always increases the surface area, if the mean curvature is nonzero, but the second term may decrease or increase it depending on the signs of the normal derivative and the mean curvature.

2.3 Solution of the area equation for material surfaces

For material surfaces Eq. 17 for the area of level surfaces is reduced to

$$\frac{\partial A_\Phi}{\partial t}(\varphi,t) = \int\limits_{S_\Phi(\varphi,t)} dA\left(\frac{\partial v_\alpha}{\partial x_\alpha} - n_\alpha n_\beta\frac{\partial v_\beta}{\partial x_\alpha}\right) \quad , \tag{22}$$

with the initial condition

$$\mathcal{A}_\Phi(\varphi,0) = \int\limits_{S_\Phi(\varphi,0)} dA \quad , \tag{23}$$

as the area of the surface $\Phi(\underline{x},0) = \varphi$. Material surfaces enjoy the property that they are the one-to-one image of the initial surfaces. It is clear that Lagrangian variables are the proper choice for the formulation of their evolution. Denoting by τ and $\underline{a}$ the Lagrangian variables defined as time and initial position of material points, the position $\underline{X}(\tau,\underline{a})$ at a later time is then the solution of

$$\frac{dX_\alpha}{d\tau} = v_\alpha(\tau,\underline{X}), \qquad X_\alpha(0,\underline{a}) = a_\alpha \quad , \tag{24}$$

where $v_\alpha(t,\underline{x})$ is the Eulerian velocity and t, $\underline{x}$ are the usual Eulerian variables. The inverse transformation (from Eulerian field to Lagrangian field) $a_\alpha = X_\alpha^{-1}(t,\underline{x})$ is unique and smooth as long as the Eulerian velocity field is smooth. The solution to Eq. 23-24 can be constructed if the co-area formula is applied

$$\mathcal{A}_\Phi(\varphi,t) = \int\limits_{\mathcal{D}} d\underline{x}|\nabla\Phi|\delta(\Phi(\underline{x},t)-\varphi) \quad ,$$

and the fact that the level surface is embedded in a part of the flow field is used. Taking for $\mathcal{D}(\tau)$ a subset of the flow field that contains the level surface at time τ and using the fact that the mapping $\underline{X}(\tau,\underline{a})$ is defined not only of the level surface but on the set $\mathcal{D}(\tau)$, we transform the volume integral to the Lagrangian frame as integral over $\mathcal{D}(0)$

$$\mathcal{A}_\Phi(\varphi,\tau) = \int\limits_{\mathcal{D}(0)} d\underline{a}J(\underline{a},\tau)|\nabla\Phi|(\underline{a},\tau)\delta(\Phi(\underline{X},\tau)-\varphi) \quad , \tag{25}$$

where J denotes the Jacobian of the transformation given by

$$J(\underline{a},\tau) = \frac{1}{6}\epsilon_{\alpha\beta\gamma}\epsilon_{\delta\eta\omega}\frac{\partial X_\alpha}{\partial a_\delta}\frac{\partial X_\beta}{\partial a_\eta}\frac{\partial X_\gamma}{\partial a_\omega} \quad . \tag{26}$$

This Jacobian is the determinant of the Lagrangian deformation tensor $J_{\alpha\beta}$

$$J_{\alpha\beta} = \frac{\partial X_\alpha}{\partial a_\beta} \quad ,$$

which is nonsingular for smooth flows with $J > 0$. The points on the level surface are materially invariant so

$$\delta(\Phi(\underline{X},\tau)-\varphi) = \delta(\Phi(\underline{a},0)-\varphi) \quad ,$$

and it follows that the area at time τ is given by

$$\mathcal{A}_\Phi(\varphi,\tau) = \int\limits_{\mathcal{D}(0)} d\underline{a}|\nabla\Phi|(\underline{a},0)\delta(\Phi(\underline{a},0)-\varphi)J(\underline{a},\tau)\frac{|\nabla\Phi|(\underline{a},\tau)}{|\nabla\Phi|(\underline{a},0)}$$

where $d\underline{a}$ is the volume differential at time zero. Application of the co-area formula leads to a surface integral over the initial surface

$$\mathcal{A}_\Phi(\varphi,\tau) = \int\limits_{S_\Phi(\varphi,0)} dA(0)J(\underline{a},\tau)\frac{|\nabla\Phi|(\underline{a},\tau)}{|\nabla\Phi|(\underline{a},0)} \quad , \tag{27}$$

where $dA(0)$ denotes the surface differential at time zero. This is the desired solution of Eq. 23 and Eq. 24, as can be verified easily by differentiation. The solution Eq. 27 can be recast in terms of the Lagrangian deformation tensor if the kinematic relation (Ottino 1989, section 2.7)

$$dA(\tau) = dA(0)J(\underline{a},\tau)\left(n_\alpha n_\beta J^{-1}_{\gamma\alpha}J^{-1}_{\gamma\beta}\right)^{\frac{1}{2}} \tag{28}$$

is applied. It follows at once that the solution Eq. 28 is thus given by

$$\mathcal{A}_\Phi(\varphi,\tau) = \int\limits_{S_\Phi(\varphi,0)} dA(0)J(\underline{a},\tau)\left(n_\alpha n_\beta J^{-1}_{\gamma\alpha}J^{-1}_{\gamma\beta}\right)^{\frac{1}{2}} \quad , \tag{29}$$

valid for material surfaces. The version Eq. 29 of the solution shows the special property of material surfaces possessing nonsingular Jacobians. This is not the case for surfaces moving relative to the fluid, and Eq. 27 and Eq. 29 are then not necessarily well defined.

It is worth noting that for incompressible flows $J = 1$ holds and, assuming constant molecular diffusivity Γ, the result

$$\mathcal{A}_\Phi(\varphi,\tau) = \int\limits_{S_\Phi(\varphi,0)} dA(0)\left(\frac{\epsilon_\Phi(\underline{a},\tau)}{\epsilon_\Phi(\underline{a},0)}\right)^{\frac{1}{2}} \tag{30}$$

follows from Eq. 27. It shows that the evolution of the area of material surfaces for incompressible flows is determined by the initial surface and the values of the scalar dissipation $\epsilon_\Phi \equiv \Gamma\nabla\Phi\cdot\nabla\Phi$ on the surface. The integral can be computed if the Lagrangian scalar dissipation $\epsilon_\Phi(\underline{a},\tau)$ is known, which is often the hard part of the problem. The expression for the area Eq. 27 does not contain any statistical information as only surface integrals are involved. It is equal to the expected area for homogeneous turbulence but is different from expected values for non-homogeneous flows.

2.4 Computation of the area of level surfaces

Consider a scalar field $\Phi(\underline{x},t) \geq 0$, such as enstrophy, temperature, density etc., that is a realization of a turbulent field. The equation of the iso-surfaces of Φ is

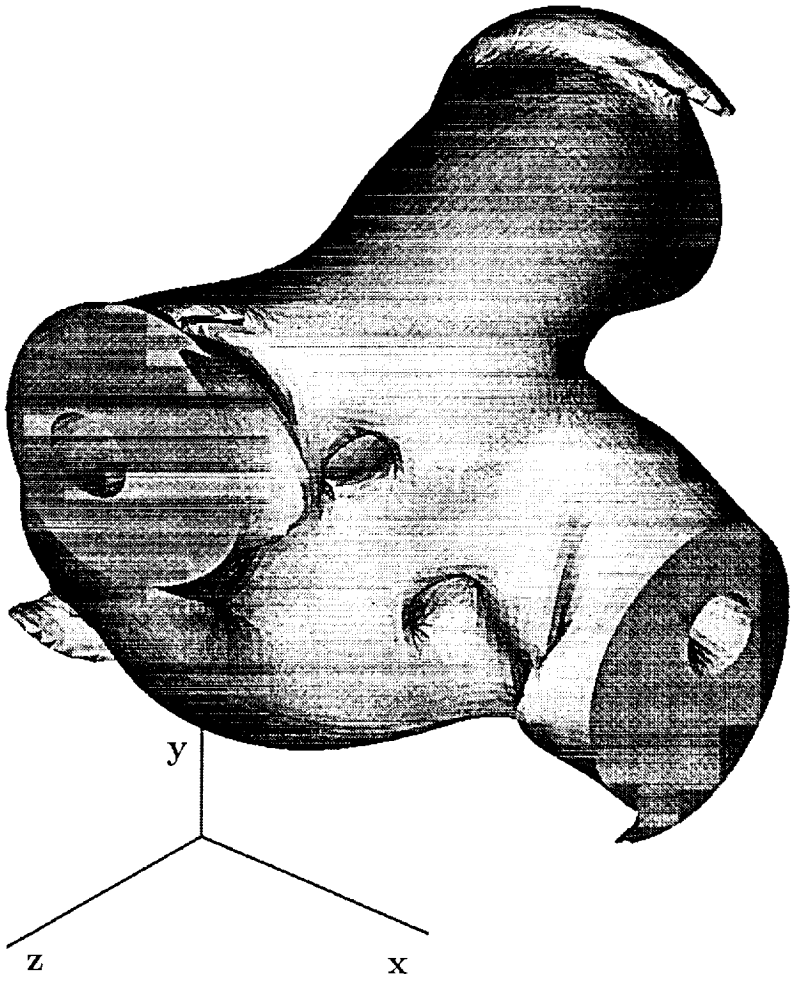

FIGURE 1. Level surface of kinetic energy for a periodic viscous flow generated by the interaction of two vortex tubes, which are initially off-set and orthogonal. The flow is used as example for the computation of the surface area.

then given implicitly by $S_\Phi(\varphi) = \{\underline{x} \in \mathcal{D} : \Phi(\underline{x}) = \varphi\}$. It follows from Eq. 2 that surface integrals can be represented as volume integrals over a fixed domain $\mathcal{D}$ (note that $S_\Phi(\varphi)$ is not the boundary of the domain $\mathcal{D}$; hence, the Gauss theorem is not applicable). The surface area is

$$\mathcal{A}_\Phi(\varphi, t) = \int_{\mathcal{D}} d\underline{x} |\nabla\Phi| \delta(\Phi(\underline{x}, t) - \varphi) \tag{31}$$

in which the Dirac-pseudofunction selects the points in space where the level surface is located. This property indicates that an integral transform with respect to the range of the scalar Φ would remove the delta function. Since the scalar Φ is

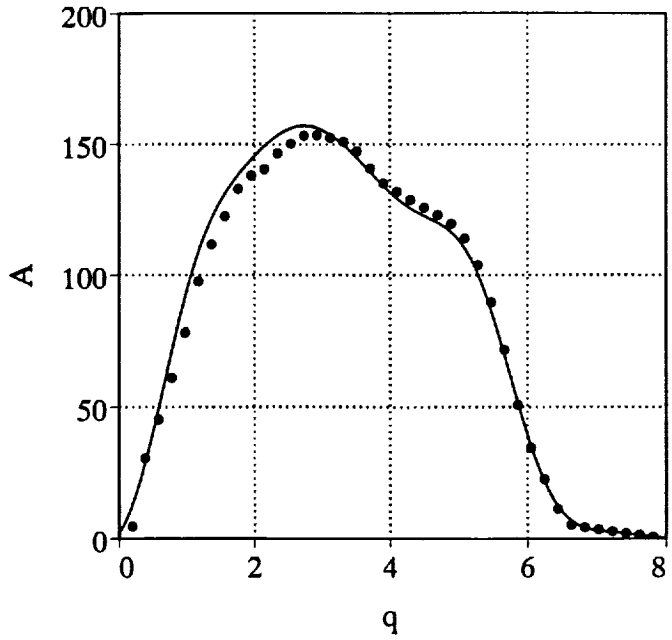

FIGURE 2. Surface area of level surfaces for the flow illustrated in Fig. 1. The symbols correspond to the triangulation method and the line to the Laplace transform method Eq. 33 and Eq. 34.

nonnegative, it follows that the Laplace transform is the appropriate tool. Hence, the transformed surface area is then defined by

$$\hat{\mathcal{A}}_\Phi(s) \equiv \int_0^\infty d\varphi \mathcal{A}_\Phi(\varphi) \exp(-s\varphi) \quad , \tag{32}$$

where $s = u + iw$ is a complex variable. Using Eq. 31 we obtain

$$\hat{\mathcal{A}}_\Phi(s) = \int_0^\infty d\varphi \exp(-s\varphi) \int_{\mathcal{D}} d\underline{x} \delta(\Phi(\underline{x}) - \varphi) |\nabla\Phi| \quad ,$$

which leads to

$$\hat{\mathcal{A}}_\Phi(s) = \int_{\mathcal{D}} d\underline{x} |\nabla\Phi| \exp(-s\Phi(\underline{x})) \quad . \tag{33}$$

This is a powerful result with both practical and theoretical implications: the Laplace transform of the surface area of level surfaces for all level values can be computed without computing the location of a single level surface. Furthermore, this computation is much more efficient than methods based on triangulation of level surfaces that keep track of the connectedness of the triangles. It is also useful for theoretical considerations since the integrand in Eq. 33 is a well defined function

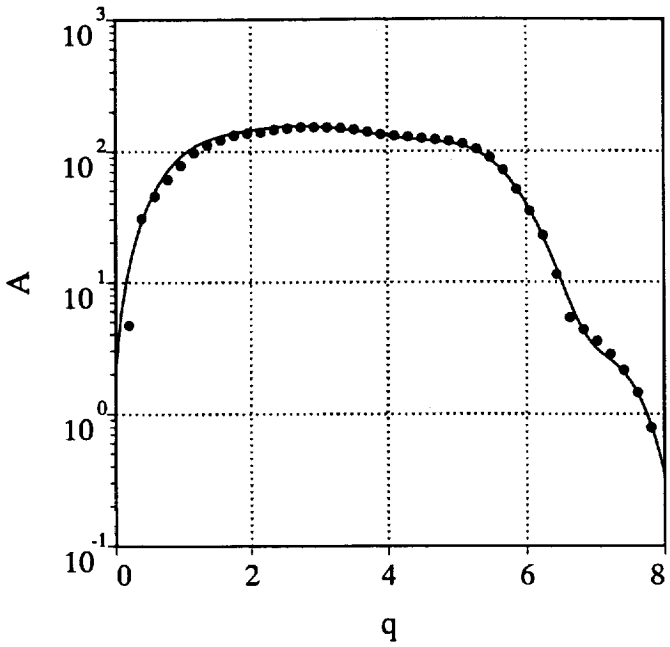

FIGURE 3. Same as Fig. 2 with logarithmic scale for the vertical axis.

for finite s and not a distribution, and is accessible to the methods of classical analysis. Once the Laplace transform has been determined, the inverse transform produces the desired surface area according to

$$\mathcal{A}_\Phi(\varphi) = \frac{1}{2\pi i} \int_{u-i\infty}^{u+i\infty} ds \hat{\mathcal{A}}_\Phi(s) \exp(s\varphi) \quad . \tag{34}$$

The numerical computation of the integrals in Eq. 33 and Eq. 34 requires some care. It is easy to see that the range of w in the independent variable $s = u + iw$ in Eq. 33 and Eq. 34 is limited by the highest wave-number that can be resolved on the lattice of discrete values of φ

$$w_{max} \| \triangle \Phi(\underline{x}, t) \| \leq \pi \quad ,$$

where $\| \cdot \|$ is an appropriate norm and $\triangle\Phi$ denotes the difference of Φ between two neighboring lattice points. Choosing w_{max} significantly larger than this limit leads to integrals over rapidly oscillating functions which diverge. For the present case the maximum norm was initially chosen, which turned out to be too restrictive, and the limit was relaxed to twice the value given above. This aspect of the transform method requires further analysis.

As an example, the scalar kinetic energy $\Phi(\underline{x}, t) \equiv q(\underline{x}, t) = v_\alpha v_\alpha$ generated as a numerical solution of the Navier-Stokes equations for the interaction of two initially orthogonally offset vortex tubes ($Re = 1500$) at time $t = 1.375$ is used to illustrate the transform method outlined above. One of the level surfaces is shown in Fig. 1 for

the level value which is 48.78% of the maximum. It has the Euler number (Kollmann and Chen 1994) $\chi = -10$, which corresponds to the genus $g = 1 - \frac{1}{2}\chi = 6$ or a sphere with six handles, and the fragmentation $N = 1$, which means that there is only one surface component. The intersections of the level surface (the flow field is periodic in all three directions) with the cubic flow domain are artificially closed with lids. The area of the lids is not included in the results for the surface area. Two methods for the computation of the surface area are applied: Triangulation of the level surfaces, which determines the connectedness information for all triangles and thus allows also the computation of the topological properties χ and N, and the Laplace transform method given by Eq. 33 and Eq. 34. The results in Fig. 2 (linear scale, the full line is the transform method and the symbols the triangulation) and Fig. 3 (semi-logarithmic plot) show that good agreement between the two methods is achieved. The advantage of the Laplace transform method becomes apparent if the CPU times are compared: The Laplace transform method (using 100 points on the φ-axis) is about 1000 times faster than the triangulation method (using 40 points).

2.5 Surface density function

In modeling purposes one wishes to seek out closed equations for point quantities that can be easily discretized and introduced in fluid mechanics codes. The density of iso-surface is introduced in this section as a quantity that characterizes, in mean, the behavior of iso-concentration surfaces for a reactive scalar field $\Phi(\underline{x})$ that follows Eq. 9.

The basic relation (Eq. 2) set out in Section 2.1 suggests that for $f = 1$ a local and instantaneous measure of the density per unit volume of iso-surface is provided by

$$\Sigma(\varphi;\underline{x},t) = |\nabla\Phi(\underline{x})|\delta(\Phi(\underline{x}) - \varphi) \quad .$$

Indeed from Eq. 2

$$\int_{\mathcal{D}} d\underline{x}\Sigma(\varphi;\underline{x},t) = \int_{S_\Phi(\varphi)} dA(\underline{x}) = \mathcal{A}_\Phi \quad , \tag{35}$$

and $\Sigma(\varphi;\underline{x},t)$ corresponds to the ratio $\frac{\delta A_\Phi}{\delta V}$ in the limit $\delta V \to 0$. This expression indicates that, within a turbulent environment, the mean surface density function (sdf) $\overline{\Sigma}(\varphi;\underline{x},t)$ is the product of the expected value for the magnitude of the gradient of $\Phi(\underline{x},t)$, conditioned on being on one iso-surface $\Phi(\underline{x},t) = \varphi$, times the probability of being on that surface. Indeed introducing the pdf of $\Phi(\underline{x},t) = \varphi$, namely $\overline{P}(\varphi;\underline{x},t) = \overline{\delta(\varphi - \Phi(\underline{x},t))}$, one may write:

$$\overline{\Sigma}(\varphi;\underline{x},t) = \overline{|\nabla\Phi(\underline{x},t)|\ \delta(\varphi - \Phi(\underline{x},t))} = \left(\overline{|\nabla\Phi(\underline{x},t)|\ \Big|\Phi(\underline{x},t) = \varphi}\right)\overline{P}(\varphi;\underline{x},t) \quad , \tag{36}$$

where $\left(\overline{\mid \nabla\Phi(\underline{x},t) \mid \left| \Phi(\underline{x},t)=\varphi \right.}\right)$ denotes a conditional average. (This definition of surface density has been previously used by Trouvé and Poinsot (1994) to evaluate flame surface density from DNS.)

All information contained in the sdf is also available through the joint pdf of Φ and its gradient; models have been proposed for this joint pdf in the case of reacting and non-reacting flows (Meyers and O'Brien 1981, Dopazo 1994, Fox 1994). The iso-surface is one of the standard concepts used to investigate complex phenomena in premixed turbulent flames (Veynante *et al.* 1994); therefore, despite the detailed statistical description involved in this joint pdf, it is interesting to restrict the present study to the specific equation for $\overline{\Sigma}(\varphi;\underline{x},t)$.

An exact transport equation for the surface density function $\overline{\Sigma}(\varphi;\underline{x},t)$ may be written (Vervisch *et al.* 1994):

$$\begin{aligned}\overline{\frac{D\Sigma(\varphi;\underline{x},t)}{Dt}} &= \left(\overline{(-\underline{n}\,\underline{n}:\nabla\underline{v}) \mid \nabla\Phi(\underline{x},t) \mid \left|\Phi(\underline{x},t)=\varphi\right.}\right)\overline{P}(\varphi;\underline{x},t) \\ &- \left(\overline{\underline{n}.\nabla\Omega_\Phi(\underline{x},t)\left|\Phi(\underline{x},t)=\varphi\right.}\right)\overline{P}(\varphi;\underline{x},t) \\ &- \frac{\partial}{\partial\varphi}\left[\left(\overline{\Omega_\Phi(\underline{x},t)\left|\Phi(\underline{x},t)=\varphi\right.}\right)\overline{P}(\varphi;\underline{x},t)\right] \quad .\end{aligned} \tag{37}$$

It is important to note that in Eq. 37 φ is an independent variable (sample space variable), and Eq. 37 is valid for all the iso-concentration surfaces defined from the progress variable field. When the various terms contributing to the sdf evolution are transposed to a surface formalism, they are equivalent to those of Eq. 4 or Eq. 17.

2.6 Unified treatment of pdf and sdf equations

Pdf modeling has been shown to be an efficient tool for the computation of turbulent non-premixed flames (Kollmann 1990, Borghi *et al.* 1991). The pdf approach has a great potential because it allows for including the description of the chemistry in a closed form, the modeling issue related to the evaluation of the mean burning rate being reduced to the estimation of the small-scale mixing. However, in the case of turbulent premixed flames, classical mixing models may fail because of the particular properties of the reactive and diffusive zones. Indeed, mixing is a prerequisite for reactions in non-premixed systems as is preheating in premixed flows; therefore, the resulting predictions depend crucially on the properties of the mixing model, no matter how accurately the chemical reactions can be represented.

The pdf equation may be written (Kollmann 1990):

$$\overline{\frac{DP(\varphi;\underline{x},t)}{Dt}} = -\frac{\partial}{\partial\varphi}\left[\left(\overline{\Omega_\Phi(\underline{x},t)\left|\Phi(\underline{x},t)=\varphi\right.}\right)\overline{P}(\varphi;\underline{x},t)\right] \quad , \tag{38}$$

where the bar over the substantial derivative indicates that turbulent transport effects are included. By introducing the dissipation of the scalar field $\epsilon_\Phi = \Gamma \mid \nabla\Phi \mid^2$,

the modification of the pdf in composition space may be written in an alternative form

$$\frac{\overline{DP(\varphi;\underline{x},t)}}{Dt} = -\frac{\partial}{\partial\varphi}\left[\left(\overline{\dot{W}_\Phi\middle|\Phi(\underline{x},t)=\varphi}\right)\overline{P}(\varphi;\underline{x},t)\right] - \frac{\partial^2}{\partial\varphi^2}\left[\left(\overline{\epsilon_\Phi\middle|\Phi(\underline{x},t)=\varphi}\right)\overline{P}(\varphi;\underline{x},t)\right] \tag{39}$$

In Eq. 39 the chemical source is closed, but the mixing term involving second order derivative in composition space is unknown when a one-point description is adopted for the turbulent flow. This term is actually representative of the distribution of the magnitude of gradient of the scalar field along the iso-concentration surfaces. It is therefore natural to look for a closure of this term that takes advantage of the information included in $\overline{\Sigma}(\varphi;\underline{x},t)$ concerning the dynamics of these iso-surfaces. This approach leads to the development of a PDF-SDF model in which a system of equations consisting of the transport equations for the pdf and the sdf is solved.

The sdf equation can be recast in a form that emphasizes the similarity to the pdf equation if a relation between conditional and surface means is established. Surface means may be defined by

$$\left(\overline{\Omega_\Phi(\underline{x},t)\middle|\mathcal{A}_{\Phi=\varphi}}\right) = \frac{\int_{\mathcal{D}} d\underline{x}\Omega_\Phi(\underline{x},t)\Sigma(\varphi;\underline{x},t)}{\int_{\mathcal{D}} d\underline{x}\Sigma(\varphi;\underline{x},t)} = \frac{1}{\mathcal{A}_\Phi}\int_{S_\Phi(\varphi)} dA(\underline{x})\Omega_\Phi(\underline{x},t) \quad , \tag{40}$$

where Eq. 2 has been used when $\Sigma(\varphi;\underline{x},t) = \mid \nabla\Phi \mid \delta(\varphi-\Phi)$ is the instantaneous surface density function.

The conditional mean of $\Omega_\Phi(\underline{x},t)$ may be written:

$$\left(\overline{\Omega_\Phi(\underline{x},t)\middle|\Phi(\underline{x},t)=\varphi}\right) = \frac{\overline{\Omega_\Phi(\underline{x},t)\delta(\Phi(\underline{x},t)-\varphi))}}{\overline{\delta(\Phi(\underline{x},t)-\varphi)}} \quad . \tag{41}$$

A relation to the surface mean can be established for homogeneous flows if the co-area formula Eq. 2 is applied to Eq. 41. It follows for homogeneous flows that the conditional mean is the ratio of volume integrals which become surface integrals using Eq. 2

$$\left(\overline{\Omega_\Phi(\underline{x},t)\middle|\Phi(\underline{x},t)=\varphi}\right) = \frac{\int_{S_\Phi(\varphi)} dA(\underline{x})\frac{\Omega_\Phi(\underline{x},t)}{\mid\nabla\Phi\mid}}{\int_{S_\Phi(\varphi)} dA(\underline{x})\frac{1}{\mid\nabla\Phi\mid}} \quad ,$$

which is recognized as the desired relation between conditional and surface means

$$\overline{\left(\Omega_\Phi(\underline{x},t)\middle|\Phi(\underline{x},t)=\varphi\right)} = \frac{\overline{\left(\frac{\Omega_\Phi(\underline{x},t)}{|\nabla\Phi|}\middle|\mathcal{A}_{\Phi=\varphi}\right)}}{\overline{\left(\frac{1}{|\nabla\Phi|}\middle|\mathcal{A}_{\Phi=\varphi}\right)}} \quad .$$

Both sides are defined for non-homogeneous flows but are not equal since the right side is the ratio of geometrical means Eq. 40 and not statistical expectations. Conversly, the surface mean can be expressed in terms of conditional means

$$\overline{\left(\Omega_\Phi(\underline{x},t)\middle|\mathcal{A}_{\Phi=\varphi}\right)} = \frac{\overline{\left(\Omega_\Phi(\underline{x},t)\mid\nabla\Phi\mid\middle|\Phi(\underline{x},t)=\varphi\right)}}{\overline{\left(\mid\nabla\Phi\mid\middle|\Phi(\underline{x},t)=\varphi\right)}} \quad , \tag{42}$$

valid for homogeneous flows.

The application of the previous results to homogeneous flows converts the sdf equation (Eq. 37) in the form

$$\frac{\partial\overline{\Sigma}(\varphi;\underline{x},t)}{\partial t} = -\frac{\partial}{\partial\varphi}\left[\overline{\left(\Omega_\Phi\middle|\mathcal{A}_{\Phi=\varphi}\right)}\,\overline{\Sigma}(\varphi;\underline{x},t)\right] + \overline{\left(\theta_s\middle|\mathcal{A}_{\Phi=\varphi}\right)}\,\overline{\Sigma}(\varphi;\underline{x},t) \quad , \tag{43}$$

where θ_s denotes the total rate of generation of surface area per unit volume

$$\theta_s = -\underline{n}\,\underline{n}:\nabla\underline{v} - \frac{1}{|\nabla\Phi|}\underline{n}.\nabla\Omega_\Phi \quad .$$

Comparison of the pdf Eq. 38 with the Eq. 43 for the mean sdf shows that the sdf is transported in scalar space by the same mechanism as the pdf, but is also created or destroyed by the tangential strain rate and by the flux of the imbalance between diffusion and reactions normal to the level surfaces.

The equations for the pdf and the sdf in homogeneous flows pose two closure problems: the fluxes in scalar space and the surface mean of the total generation rate of the sdf. The particular structure of premixed flames and the previous analysis suggests dealing with mixing and chemical reactions in a unified way by developing a closure model for their combined effects. Pdf and sdf are moved in scalar space by the conditional mean and the surface mean of the same quantity, namely the imbalance between diffusion and reactions.

3. The internal structure of premixed turbulent flames (DNS)

A database of turbulent premixed flames has been generated by using a fully compressible direct numerical simulation code (Guichard, Vervisch and Domingo 1994). These simulations are three dimensional, and fields are computed by using a 129x129x129 grid. The numerical approach chosen has been proposed by Lele (1990), Poinsot and Lele (1992).

FIGURE 4. Snapshots of the flame surface contour ($\varphi = 0.8$).

In previous studies of premixed and non-premixed turbulent flames at CTR (Trouvé and Poinsot 1994, Vervisch 1992), initial conditions were generated by using a laminar and planar flame on which a homogeneous turbulent field was superimposed. As a consequence, prior to being distorted by the turbulence, the structure of the reactive zone corresponded to the one of a laminar flame. Globally, the computational domain was divided into fresh and burnt gases separated by a propagating turbulent flame. These simulations have been proven to be an efficient tool for studying, through the flame brush, the topology of one iso-surface identified as the flame-surface and corresponding to the location of intense reactive activity.

In order to increase the number of possibilities of sampling for all the values of the progress variable field, in the present simulations the initial scalar field is prescribed according to a pdf and to a turbulent spectrum. It is then possible to generate as initial condition a homogeneous progress variable field with pockets of burnt gases and fresh gases. A turbulence velocity field is added to this scalar field, and turbulence is allowed to decay. These pockets are convected by the turbulence, and reactive layers are created. To avoid spurious effects that can emerge from this initial condition, the procedure used to initialize the scalar field insures that the transition between fresh and burnt gases is achieved according to a smooth distribution. Non-reflecting boundary conditions are used on each side of the computational domain, and pressure waves can leave this domain.

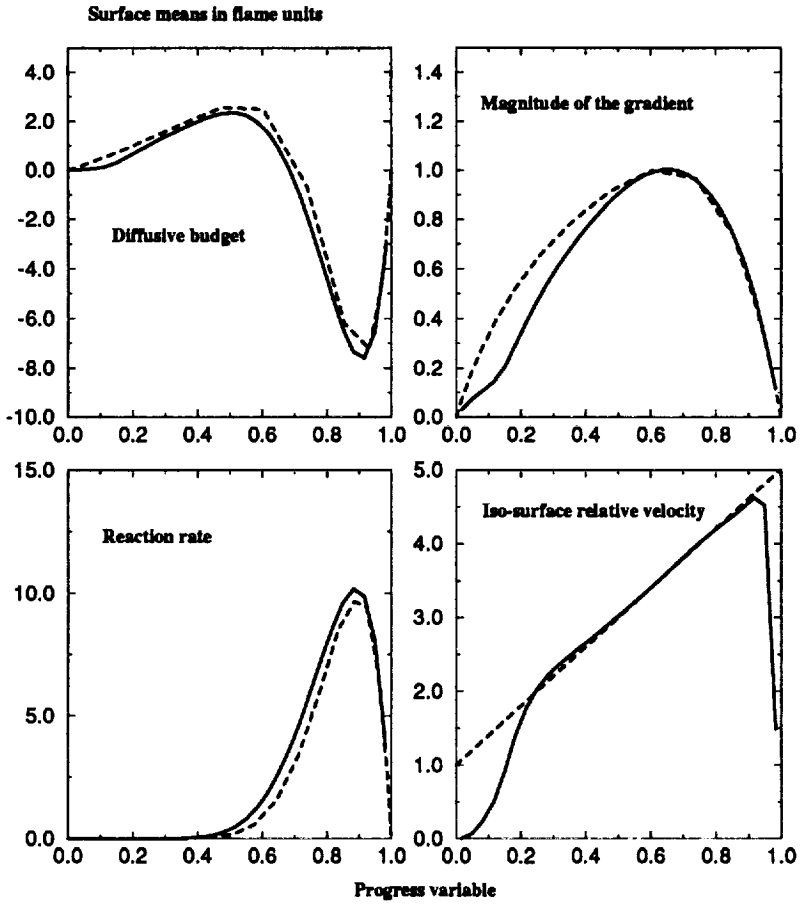

FIGURE 5. Distribution in progress variable space of surface means. ——— : turbulent flame; ---- ; laminar flame.

From the initial condition, the progress variable field is convected by the turbulence, and propagation of premixed flames is observed. A single-step chemistry with a reaction rate cast in the form of an Arrhenius law represents the chemical activity. The ratio of temperature between burnt and fresh gases is five, the Zeldovich number has a value of eight. The initial ratio between the rms turbulent velocity and laminar flame speed is the order of three, and the value of the Damköhler number based on the Kolmogorov time scale and the laminar flame time is about unity. The initial turbulent Reynolds number based on the integral length scale is about seventeen, while the Reynolds number based on the initial Taylor microscale is about fifteen. The formalism which has been developed above is used to analyze data from this calculation.

After one flame time, the flame surface exhibits a very complex and convoluted shape that can be observed in Fig. 4.

Fig. 5 presents the distribution in progress variable space of surface means as

defined in Eq. 40 for various quantities; their corresponding distribution across a one-dimensional steady unstrained laminar flame is also plotted. The distribution of surface means for the diffusive budget of the progress variable $\frac{1}{\rho}(\nabla.(\rho\Gamma\nabla\Phi(\underline{x},t)))$, of the chemical source $\dot{W}_\Phi$, and of the magnitude of the gradient $\mid \nabla\Phi(\underline{x},t) \mid$ follow the laminar response except in the preheat zone ($\Phi < 0.5$), where, because of the turbulence activity, the flame is not able to sustain the flamelet structure. The turbulence clearly affects the progress variable gradient in the preheating region. As a consequence, the surface mean of the iso-surface relative progression velocity

$$V = \frac{1}{\rho|\nabla\Phi|}\frac{\partial}{\partial x_\alpha}(\rho\Gamma\frac{\partial\Phi}{\partial x_\alpha}) + \frac{1}{|\nabla\Phi|}\dot{W}_\Phi = \frac{1}{\mid\nabla\Phi\mid}\Omega_\Phi \quad ,$$

drops in the preheat zone and in the burnt gases. One may observe with the help of these plots how the imbalance between chemical source and diffusion leads to the propagation of the various iso-surfaces. However, even though the surface mean value of this velocity is close to the laminar flamelet value, the scatter plot (Fig. 6) of this quantity shows that locally the effect of the turbulence can be very large in this DNS. This result suggests that there is not a unique deterministic relationship between progress variable and propagation speed. The same observation has been made in connection with the imbalance between reaction and diffusion as well as for the magnitude of the gradient.

Fig. 6 also displays the pdf of the progress variable at time $t = 0$ and the pdf after one flame time; a bimodal shape is observed in accordance with the existence of the flamelets seen in Fig. 5. The effects of the turbulence on the preheating zone is emphasized in Fig. 6 where the area of the iso-surface is increased for small value of the progress variable.

All of these observations suggest the existence of a flamelet zone within the turbulent flame brush, where mean conditional surface values follow the laminar flame structure. However, the existence of a preheating region is also observed, and the properties of the mixing in this zone may control the behavior of the entire flame structure.

The total flame stretch, defined for the iso-surface corresponding to the progress variable that gives the peak value of the reactive activity, is at a time in the simulation corresponding to Fig. 5 and Fig. 6 positive when the mean value for the progress variable evaluated over all the computational domain is $\overline{\Phi} = 0.55$. Flame stretch is known from DNS or experimental observation (Trouvé and Poinsot (1994) Veynante *et al.* 1994) to evolve from positive to negative values as a function of the mean progress variable. In accordance with these observations, later in time, flame stretch becomes negative when the mean value of the progress variable within the domain becomes larger.

4. PDF-SDF modeling

DNS observation suggests that the premixed turbulent flame may be organized in progress variable space in three zones: a preheat zone and a burnt gas zone where mixing needs to be treated separately from the slow chemical reaction, and

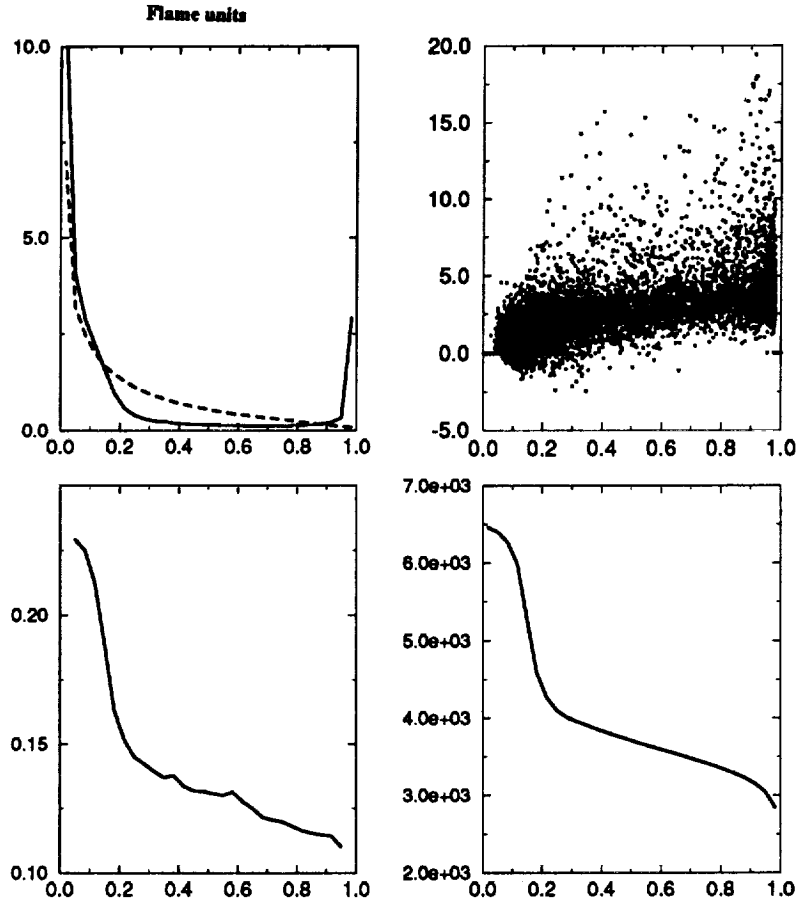

FIGURE 6. Clockwise from upper left: Pdf of the progress variable (——— , pdf; ---- , initial pdf), scatter plot of iso-surface relative progression velocity, area of iso-surfaces, and iso-surface density function.

a flamelet zone where the mean conditional surface value of the velocity of the iso-surface meets the one of a laminar flame and where laminar flamelet behavior may be invoked. Because of the necessity of introducing the chemical rate within both the preheat and burnt gases zones, Eq. 39 is appropriated for the pdf, while Eq. 38 is well suited for the flamelet zone where the convection in composition space will be deduced from flamelet behavior and $\overline{\Sigma}(\varphi; \underline{x}, t)$ represents the laminar flamelet isosurface density. It is zero when no laminar flamelet burning zone exists.

A direct approach to close the pdf equation can be developed by prescribing for the imbalance Ω_Φ the value corresponding to the planar unstrained laminar flame $\Omega_{\Phi_{fl}}$. When combining $\Omega_{\Phi_{fl}}$ with a classical mixing model, a closed pdf mixing term emerges (Anand and Pope 1987). Here, our objective is to take advantage of both pdf and sdf transport equations at the same time. The value of Ω_Φ corresponding to the laminar flamelet structure will be used, but in conjunction with strain-rate curvature and related mixing effects in both pdf and sdf equations.

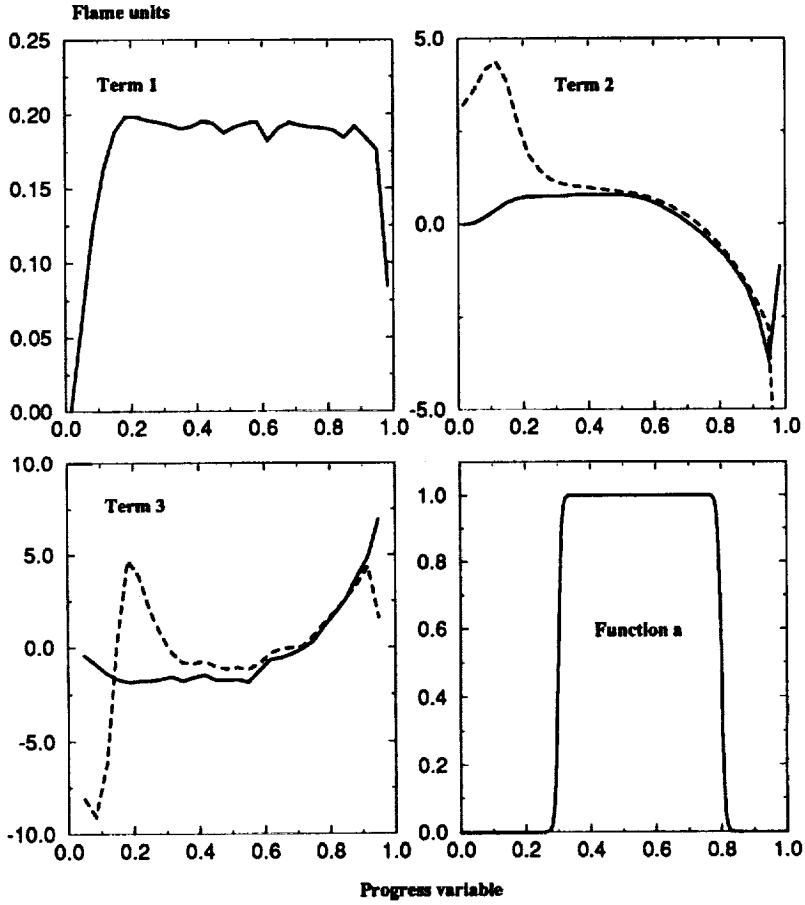

FIGURE 7. Comparison between modeled sdf terms (valid within the flamelet range) and DNS. ——— : DNS; ---- : proposed model.

4.1 Modeling for the sdf equation

In this work, the turbulent convection will not be considered and its investigation may be found in this book elsewhere (Trouvé *et al.* 1994).

From the above analysis, the equation for the flamelet sdf

$$\overline{\Sigma}(\varphi;\underline{x},t) = \left(\overline{|\nabla\Phi| \,\middle|\, \Phi(\underline{x},t)=\varphi}\right)\overline{P}(\varphi;\underline{x},t) \quad , \tag{44}$$

may be written:

$$\frac{\partial\overline{\Sigma}(\varphi;\underline{x},t)}{\partial t} + \overline{\nabla.(\Sigma(\varphi;\underline{x},t)\mathbf{v})} = \underbrace{\left(\overline{\phi_s \,\middle|\, \mathcal{A}_{\Phi=\varphi}}\right)}_{\text{Term 1}}\overline{\Sigma}(\varphi;\underline{x},t)$$

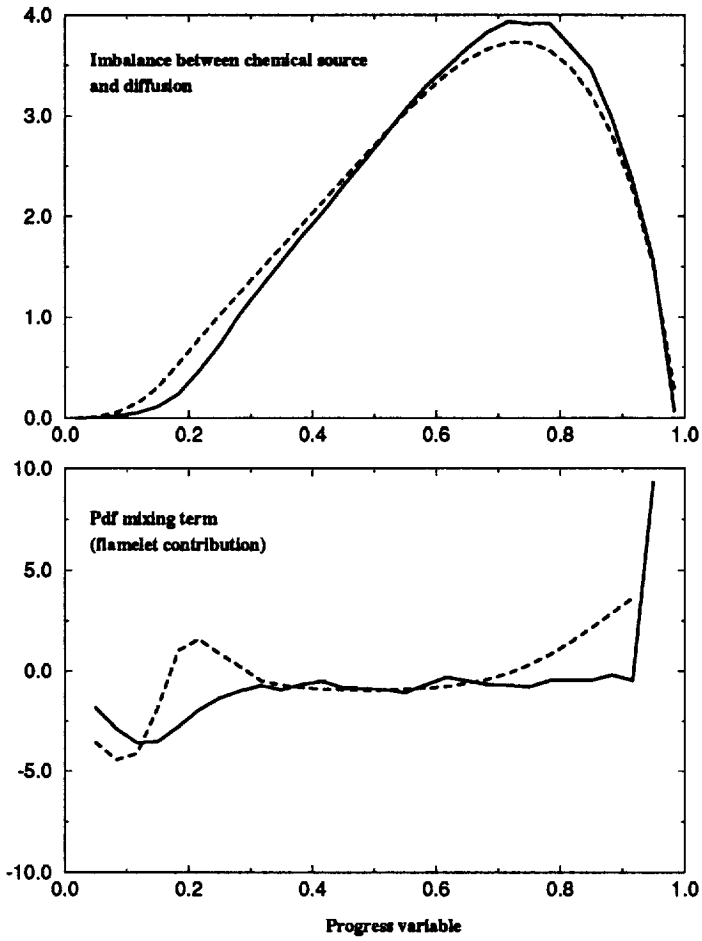

FIGURE 8. Comparison between modeled pdf terms (valid within the flamelet range), top, and DNS (flame units), bottom. Top: ——— , conditional mean value; ---- , conditional surface mean value. Bottom: ——— , DNS; ---- , proposed model.

$$\underbrace{-\left(\overline{\underline{n}.\nabla\Omega_\Phi(\underline{x},t)\Big|\Phi(\underline{x},t)=\varphi}\right)\overline{P}(\varphi;\underline{x},t)}_{\text{Term 2}} \qquad (45)$$

$$\underbrace{-\frac{\partial}{\partial\varphi}\left[\left(\overline{\Omega_\Phi(\underline{x},t)\mid\nabla\Phi(\underline{x},t)\mid\Big|\Phi(\underline{x},t)=\varphi}\right)\overline{P}(\varphi;\underline{x},t)\right]}_{\text{Term 3}} \quad .$$

The strain rate term $\left(\overline{\phi_s\Big|\mathcal{A}_{\Phi=\varphi}}\right)$ is representative of a physical process that affects in a similar way all the iso-surfaces of the scalar field. As presented in Fig. 7 (Term 1) this contribution does not strongly depend on the progress variable. Therefore, it is possible to speculate that model closures developed for the in-plane

strain rate in the framework of the flame-surface density approach can be extended to the sdf equation (Meneveau and Poinsot 1991). Attention will be especially focused on Term 2 and Term 3.

For Term 2 one may prove that the expression

$$-\left(\overline{\underline{n}.\nabla\Omega_\Phi(\underline{x},t)\Big|\Phi(\underline{x},t)=\varphi}\right) \quad ,$$

does not explicitly contain curvature effects (Vervisch *et al.* 1994). The contribution of curvature of the field is actually present through the pdf $\overline{P}(\varphi;\underline{x},t)$ that multiplies this term in the sdf budget. Hence it is possible to build a closure by using the flamelet structure. If $S_{fl}(\varphi)$ denotes the known laminar flame speed, evaluated in the premixed laminar unstrained flame as

$$S_{fl}(\varphi)=\frac{\Omega_\varphi}{\mid\nabla\varphi\mid}=\frac{\Omega_\varphi}{G(\varphi)} \quad ,$$

where $G(\varphi)$ is the known magnitude of the gradient of the progress variable within the laminar flame, then one may write:

$$-\left(\overline{\underline{n}.\nabla\Omega_\Phi(\underline{x},t)\Big|\Phi(\underline{x},t)=\varphi}\right)\overline{P}(\varphi;\underline{x},t)\simeq\overline{P}(\varphi;\underline{x},t)G(\varphi)\frac{\partial}{\partial\varphi}\Big(S_{fl}(\varphi)G(\varphi)\Big) \quad .$$

Evaluated from DNS the exact expression (left side) and the proposed model (right side) are displayed in Fig. 7 (Term 2). Good agreement is found according to a possible definition of the flamelet range $[\varphi_0,\varphi_1]=[0.4,0.8]$.

The same approach is followed for Term 3, and this leads to

$$-\frac{\partial}{\partial\varphi}\left[\left(\overline{\Omega_\Phi\mid\nabla\Phi\mid\Big|\Phi)=\varphi}\right)\overline{P}(\varphi;\underline{x},t)\right]\simeq-\frac{\partial}{\partial\varphi}\Big[S_{fl}(\varphi)G^2(\varphi)\overline{P}(\varphi;\underline{x},t)\Big] \quad .$$

The validity of this modeled expression within the flamelet range is evaluated in Fig. 7 (Term 3). One may note from Fig. 5 that according to the distribution of the progress variable gradient, flamelet range could be $[\varphi_0,\varphi_1]=[0.6,1]$ while the iso-surface relative progression velocity follows flamelet behavior for the range $[0.4,0.8]$. The same trend is observed in Fig. 7 where the modeled term related to the propagation (Term 2) follows its exact DNS expression in the range $[0.4,0.8]$, while good agreement is obtained for the closure related to mixing in the range $[0.6,0.8]$.

The closed transport equation for the sdf is only valid within the flamelet zone; however, information coming from the preheat and burnt gases zones is present through the pdf $\overline{P}(\varphi;\underline{x},t)$. The partially closed equation contains one source term and one term representing transport in composition space and reads:

$$\frac{\partial\overline{\Sigma}(\varphi;\underline{x},t)}{\partial t}+\overline{\nabla.(\Sigma(\varphi;\underline{x},t)\mathbf{v})}=\left(\overline{\phi_s\Big|\mathcal{A}_{\Phi=\varphi}}\right)\overline{\Sigma}(\varphi;\underline{x},t)$$
$$-\mathcal{W}(\varphi_0,\varphi_1)\left(\frac{1}{2}\overline{P}(\varphi;\underline{x},t)S_{fl}(\varphi)\frac{\partial}{\partial\varphi}G^2(\varphi)+S_{fl}(\varphi)G^2(\varphi)\frac{\partial}{\partial\varphi}\overline{P}(\varphi;\underline{x},t)\right), \tag{46}$$

where the turbulent transport effects are included in the second term on the left hand-side. The function $\mathcal{W}(\varphi_0,\varphi_1)$ insures that when flamelets are not present the RHS of Eq. 46 goes to zero ($\mathcal{W}(\varphi_0,\varphi_1)$ is equal to zero when the flamelet range $[\varphi_0,\varphi_1]$ is not defined and unity when flamelets are present).

4.2 Modeling for the pdf equation

To treat both flamelet part and mixing zones, from Eq. 38 and Eq. 39 the exact transport equation for the pdf may be cast in the form

$$\begin{aligned}\overline{\frac{DP(\varphi;\underline{x},t)}{Dt}}&=-a(\varphi;\underline{x},t)\frac{\partial}{\partial\varphi}\left[\left(\overline{\Omega_\Phi(\underline{x},t)\Big|\Phi(\underline{x},t)=\varphi}\right)\overline{P}(\varphi;\underline{x},t)\right]\\&-(1.-a(\varphi;\underline{x},t))\frac{\partial}{\partial\varphi}\left[\left(\overline{\dot{W}_\Phi\Big|\Phi(\underline{x},t)=\varphi}\right)\overline{P}(\varphi;\underline{x},t)\right]\\&-(1.-a(\varphi;\underline{x},t))\frac{\partial^2}{\partial\varphi^2}\left[\left(\overline{\epsilon_\Phi\Big|\Phi(\underline{x},t)=\varphi}\right)\overline{P}(\varphi;\underline{x},t)\right],\end{aligned} \tag{47}$$

where $a(\varphi;\underline{x},t)$ is a smooth function equal to unity in the flamelet zone of φ space and to zero in the outer flamelet regions. A possible shape for the function a is proposed in Fig. 7. The way in which the flamelet range $[\varphi_0(\underline{x},t),\varphi_1(\underline{x},t)]$ is to be determined will be considered later.

Within the out-of-flamelet zone, a classical mixing modeling (Kollmann 1990) can be used with complex chemistry to evaluate the contribution of the reactive activity.

In the flamelet zone, from Fig. 8 it is observed that the surface mean of the imbalance Ω_Φ is almost equal to its conditional mean; from this we deduce the following modeled expression for the flamelet part of the pdf equation

$$\left(\overline{\Omega_\Phi\Big|\Phi(\underline{x},t)=\varphi}\right)\simeq\left(\overline{\Omega_\Phi\Big|\mathcal{A}_{\Phi=\varphi}}\right)=\frac{\overline{\Omega_\Phi\Sigma(\varphi;\underline{x},t)}}{\overline{\Sigma}(\varphi;\underline{x},t)}\simeq S_{fl}(\varphi)G^2(\varphi)\frac{\overline{P}(\varphi;\underline{x},t)}{\overline{\Sigma}(\varphi;\underline{x},t)},$$

and hence

$$-\frac{\partial}{\partial\varphi}\left[\left(\overline{\Omega_\Phi\Big|\Phi=\varphi}\right)\overline{P}(\varphi;\underline{x},t)\right]\simeq-\left(\frac{1}{\overline{\Phi}\,(1-\overline{\Phi})}\right)\frac{\partial}{\partial\varphi}\left[S_{fl}(\varphi)G^2(\varphi)\frac{\overline{P}^2(\varphi;\underline{x},t)}{\overline{\Sigma}(\varphi;\underline{x},t)}\right], \tag{48}$$

is introduced as a closure in Eq. 47. The validity of this expression is evaluated against the DNS results in Fig. 8.

The determination of this flamelet range is still unproven at this stage. However, we speculate that a criterion based on the imbalance between the reactive-mixing terms and the flamelet term (Eq. 48), both present in the pdf equation, may emerge to determine dynamically the values $\varphi_0(\underline{x},t)$ and $\varphi_1(\underline{x},t)$.

The partially closed system may be written:

$$\left\{\begin{array}{l} \dfrac{\partial\overline{\Sigma}(\varphi;\underline{x},t)}{\partial t} + \overline{\nabla.(\Sigma(\varphi;\underline{x},t)\mathbf{v})} = \left(\overline{\phi_s\Big|\mathcal{A}_\Phi=\varphi}\right)\overline{\Sigma}(\varphi;\underline{x},t) \\ \qquad\qquad - \mathcal{W}(\varphi_0,\varphi_1)\left(\dfrac{1}{2}\overline{P}(\varphi;\underline{x},t)S_{fl}(\varphi)\dfrac{\partial}{\partial\varphi}G^2(\varphi) + S_{fl}(\varphi)G^2(\varphi)\dfrac{\partial}{\partial\varphi}\overline{P}(\varphi;\underline{x},t)\right) \\ \overline{\dfrac{DP(\varphi;\underline{x},t)}{Dt}} = -a(\varphi;\underline{x},t)\left(\dfrac{1}{\overline{\Phi}(1-\overline{\Phi})}\right)\dfrac{\partial}{\partial\varphi}\left[S_{fl}(\varphi)G^2(\varphi)\dfrac{\overline{P}^2(\varphi;\underline{x},t)}{\overline{\Sigma}(\varphi;\underline{x},t)}\right] \\ \qquad\qquad - (1.-a(\varphi;\underline{x},t))\dfrac{\partial}{\partial\varphi}\left[\left(\overline{\dot{W}_\Phi\Big|\Phi(\underline{x},t)=\varphi}\right)\overline{P}(\varphi;\underline{x},t)\right] \\ \qquad\qquad - (1.-a(\varphi;\underline{x},t))\dfrac{\partial}{\partial\varphi}\left[\left(\dfrac{\overline{\Phi}-\varphi}{\tau_t}\right)\overline{P}(\varphi;\underline{x},t)\right] \quad , \end{array}\right.$$

in which closed expressions for the strain rate and for turbulent transport remain to be included. The LMSE (or IEM) mixing model (Dopazo 1994) has been chosen for the outer flamelet zone and τ_t is a characteristic mixing time scale. Monte, Carlo simulation is appropriated for the pdf equation (Pope 1985), while a continuous solution can be considered for a determinate numbers of bins for which the sdf equation is solved.

5. Conclusion

Because the motion of iso-surfaces is strongly connected with the transport phenomena at all scales of the turbulent flow, the behavior of scalar iso-surfaces in multi-component reacting mixture is a topic of fundamental interest. It is possible to develop some mathematical tools that describe the properties of these surfaces. In particular, a transport equation for global variable has been established and a solution for material surfaces evolution has been proposed. When introducing a surface density function, a possible link between the well-known pdf approach for turbulent combustion modeling and surface modeling emerges. From this point an attempt is made to develop a unified treatment of pdf and sdf for premixed turbulent flames. Direct numerical simulations results are used to analyze the internal structure of turbulent premixed flames and to estimate the validity of the proposed modeling.

Acknowledgements

The authors would like to thank their CTR hosts G. Ruetsch and J.-M. Samaniego for helpful assistance. J. Réveillon and L. Guichard are thanked for their help in the

development of the DNS database. Authors have benefited from many discussions with the participants of the "combustion group" during the CTR summer program.

REFERENCES

ANAND, M. S., POPE, S. B. 1987 Calculations of premixed turbulent flames by pdf methods. *Comb. and Flame.* **67,** 127-142.

BORGHI, R. 1988 Turbulent combustion modeling. *Progr. Energy Comb. Sci..* **14.**

BORGHI, R., VERVISCH, L., GARRÉTON D. 1991 The calculation of local fluctuations in non-premixed turbulent flames. *(Eds. Carvalho M. G., Lockwood, F., Taine, J.), Springer Verlag, 83-113.*

BRAY, K. N. C. 1990 Studies of the turbulent burning velocity. *Proc. R. Soc, Lond.* A, 431, 315-335.

CANDEL, S. M., POINSOT, T. J., 1990 Flame stretch and the balance equation for the flame area. *Combust. Sci. and Tech.* **70,** 1-15.

CONSTANTIN, P. 1992 Remarks on the Navier-Stokes equations. To appear.

DOPAZO, C. 1994 Recent developments in pdf methods. In *Turbulent Reacting Flows* (Eds P. A. Libby and F. A. Williams), Academic Press London, 375-474.

FOX, R. O. 1994 Improved Fokker-Planck model for the joint scalar, scalar gradient pdf. *Phys. of Fluid.* **6** (1), 334-348.

GUICHARD, L., VERVISCH, L., DOMINGO, P. 1994 Numerical study of the interaction between a mixing zone and a pressure discontinuity. *AIAA 95-0877,* to be published.

KOLLMANN, W. 1990 The pdf approach to turbulent flow. *Theoret. Comput. Fluid Dynamics.* **1,** 249-285.

KOLLMANN, W., CHEN, J. H. 1994 Dynamics of the flame surface area in turbulent non-premixed combustion. *Twenty-Fifth International Symp. on Comb.*

LELE, S. K. 1990 Compact finite difference schemes with spectral like resolution. Center for Turbulence Research, Stanford Univ./NASA Ames, Manuscript 107.

MENEVEAU, C., POINSOT, T. 1991 Stretching and quenching of flamelets in premixed turbulent combustion. *Comb. and Flame.* **86,** 3311-332.

MEYERS R. E., O'BRIEN, E. E. 1981 The joint Pdf of scalar and its gradient at a point in a turbulent fluid. *Comb. Sci and Tech.* **26,** 123-134.

MARBLE, F. E., BROADWELL, J. E. 1977 The coherent flame model for turbulent chemical reactions. *Project Squid Report,* TRW-9-PU, TRW, EI Secundo.

MAZ'JA, V. G. 1985 Sobolev spaces. *Springer V. Berlin.*

OTTINO, J. M. 1989 The kinematics of mixing: Stretching, chaos and transport. *Cambridge Texts in Applied Mathematics,* Cambridge University Press 1989.

POCHEAU, A. 1992 Front propagation in a turbulent medium. *Europhys. Lett.* **20** (5),, 401-406.

POINSOT, T., LELE, S. K. 1992 Boundary conditions for direct simulations of compressible viscous flows. *J. Comput. Phys.* **101**(1), July 92.

POPE, S. B. 1985 Pdf method for turbulent reacting flows. *Comb. Sci. and Tech.* **11**, 119-195.

TROUVÉ, A., POINSOT, T. 1994 The evolution for the flame surface density in turbulent premixed combustion. *J. Fluid Mech.* To be published.

TROUVÉ, A., VEYNANTE, D., BRAY, K. N. C., MANTEL, T. 1994 The coupling between flame surface dynamics and species mass conservation in premixed turbulent combustion. In *Proceedings of the 1994 CTR Summer Program,* Center for Turbulence Research, NASA Ames/Stanford Univ.

VEYNANTE, D., DUCLOS, J. M., PIANA, J. 1994 Experimental analysis of flamelet models for premixed combustion. *Twenty-Fifth International Symp. on Comb.*

VERVISCH, L, BIDAUX, E., BRAY, K. N. C., &, KOLLMANN, W. 1994 The transport equation for an iso-surface density function. Submitted to *Phys. of Fluids.*

VERVISCH, L. 1993 Study and modeling of finite-rate chemistry effects in turbulent non-premixed flames. *Annual Research Briefs 1992.* CTR, Stanford U./NASA Ames.